

Calculation of elastic modules behind strong shock wave

E I Kraus and I I Shabalin

Institute of Theoretical and Applied Mechanics of the Siberian Branch of the Russian Academy of Sciences, Institutskaya 4/1, Novosibirsk 630090, Russia

E-mail: kraus@itam.nsc.ru

Abstract. As part of a unified system of the few-parameter equation of state, an approach is implemented to calculate the mechanical properties of materials behind the front of strong shock waves. For aluminum and copper, the results of calculations are compared with the experimental data available for high energy densities; a close match is observed.

1. Introduction

The elastic-plastic problem is solved using the equations of conservation of mass, impulse and energy. The right sides of the equations of motion are gradients of stress tensor components, and the main diagonal contains the pressure values. While the pressure change is easily calculated using the few-parameter equation of state, the change in the deviator part of the stress tensor in the deformation process is to be determined. The deviator part of the stress tensor depends on the mechanical characteristics, which are functions of pressure and temperature. At that, one needs to understand well that the propagation of shock waves is of exceptional complexity in the deforming bodies, especially if the latter have a limited size. This complexity is because when propagating in the objects of limited size, the stress waves experience multiple reflections from the boundary surfaces of the body and interact to form a very complex wave pattern inside the object. Moreover, during the loading process, the temperature increases behind the shock wave front, and, therefore, the second and further shock waves (because of interference or reflection) propagate through the warmed-up body.

The objective of this work was to study the existing models and methods for the description of the temperature dependences of the mechanical constants of the substance, such as Young's modulus, shear modulus, and Poisson's ratio, on which basis it was required to propose a method for calculating the mechanical parameters based on the temperature and pressure, that would allow one to make the description of the stress-strain state of the material essentially more realistic.

2. The few-parameter equation of state

We consider [1] the three-term Mie–Grüneisen equation of state with the solid-phase free energy being determined as

$$F(V, T) = E_x(V) + c_{v,l} T \ln \left(\frac{\theta(V)}{T} \right) - \frac{1}{2} c_{v,e0} T^2 \left(\frac{V}{V_0} \right)^{2/3}, \quad (1)$$



where V is the specific volume, $E_x(V)$ is the “cold” energy, T is the temperature, $c_{v,l} = 3R/A$ is the specific heat of the lattice at constant volume, A is the mean atomic weight, R is the gas constant, $\theta(V)$ is the Debye temperature, and $c_{v,e0}$ is the experimental value of the electron heat capacity under standard conditions. The elastic (cold) component of energy $E_x(V)$ is related exclusively to interaction forces between the body atoms and is equal (including the energy of zero vibrations) to the specific internal energy at the absolute zero temperature.

The thermodynamic model of the few-parameter equation of state is based on the dependence of the Grüneisen parameter γ on the volume [2]

$$\gamma(V) = \frac{2}{3} - \frac{2}{(1 - aV_0/V)}a = 1 + \frac{2}{(\gamma_s - 2/3)} + \frac{2P_{t,0}}{K_s}, \quad (2)$$

where $\gamma_s = \beta K_s V_0 / c_v$, K_s is the adiabatic modulus of volume compression, c_v is the specific heat at constant volume, and $P_{t,0}$ is the thermal pressure in the initial state.

The general expression for the volume dependence of the Grüneisen parameter has the form

$$\gamma(V) = -\left(\frac{2-t}{3}\right) - \frac{V}{2} \left[\frac{d^2}{dV^2} \left(P_x V^{\frac{2t}{3}} \right) / \frac{d}{dV} \left(P_x V^{\frac{2t}{3}} \right) \right]. \quad (3)$$

In equation (3), the situation value corresponds to the Landau–Slater theory [3, 4] at $t = 0$, to the Dugdale–McDonald theory [5] at $t = 1$, and to the free-volume theory [6] at $t = 2$.

To determine the zero isotherm, we equated the expression for the Grüneisen parameter (2) at the zero temperature ($T = 0$ K) to the expression for the generalized Grüneisen parameter

$$\frac{2}{3} - \frac{2}{1 - a_x V_0/V} = -\left(\frac{2-t}{3}\right) - \frac{V}{2} \left[\frac{d^2}{dV^2} \left(P_x V^{\frac{2t}{3}} \right) / \frac{d}{dV} \left(P_x V^{\frac{2t}{3}} \right) \right]. \quad (4)$$

Here, a_x is the value of the parameter $a|_{T=0}$ at the zero temperature in equation (2), which can be taken $a_x = a(0) = 1 + 2/(\gamma_s - 2/3)$ as the first approximation.

The differential equation (4) has an analytical solution for “cold” pressure and energy

$$P_x(V) = C_1 V^{-2t/3} + C_2 H_2(V), E_x(V) = -\left(C_1 V^{1-2t/3} / (1 - 2t/3) + C_2 H_1(V) \right) + C_3. \quad (5)$$

Using the definition of the Grüneisen parameter in the Debye approximation

$$\gamma = -(d \ln \theta / d \ln V)|_T$$

and equation (2), we obtain the characteristic Debye temperature on the volume

$$\theta(V) = \theta_0 \left[\frac{(a - V/V_0)}{(a - 1)} \right]^2 \left(\frac{V_0}{V} \right)^{\frac{2}{3}},$$

where $\theta_0 = \theta(V_0)$ is the Debye temperature at the initial conditions.

The constants for equation (5) were determined and calculated in [1]. It was also demonstrated there that the set of semi-empirical relations (1)–(5) describes the behavior of thermodynamic properties of solids within 5–10% in a wide range of pressures and temperatures. For the equation of state to be applied, it is sufficient to know only six constants V_0 , β , K_t , c_v , Θ_0 , and $c_{v,e0}$ corresponding to the values of these quantities under standard conditions, which can be found in reference books on physical and mechanical properties of substances.

Thus, a simple caloric model of the equation of state without the effect of melting was proposed in [1] and successfully implemented in [7–9] for solving the high-speed dynamic problems.

In the few-parameter equation of state, the elastic properties [1] of the substance are characterized by a single value—compressibility, which determines the speed of sound

$$C^2 = \left(\frac{\partial P}{\partial \rho} \right)_S. \quad (6)$$

In studying the shock impact and application of the few-parameter equation of state, we assume that the pressure in the compressed material is isotropic and has the hydrostatic nature. The increase in density is seen in this case because of hydrostatic compression of the substance. However, this can be done only when the pressure is sufficiently large, and the effects associated with the strength of solid bodies and the existence of shear stress and strain do not play any role. If the load is small, it is necessary to take into account the elastic properties of solids. This significantly affects the nature of the dynamic processes and, in particular, the propagation of elastic compression and rarefaction waves.

In [10–12], it was shown experimentally that the strength properties of the material largely determine the nature and parameters of the rarefaction wave, propagating through the shock-compressed material, and attenuation parameters of the shock waves. One of the characteristic properties of solids, distinguishing it from the liquid is the shape stability of a solid, resistance to shear. In the fluid, there is no resistance to shear, the liquid assumes easily any shape, providing the volume does not change, i.e., liquid is characterized by zero shear modulus. At that, the stress tensor is diagonal in any coordinate system, with all three of its normal components equal to the pressure that is isotropic. The elastic properties of the fluid are characterized only by its compressibility or bulk modulus. It is known that at sufficiently high stress, the solid changes its elastic properties and become plastic, yielding, like a liquid in some aspects.

With increase of the pressure and temperature behind the shock front, elastic and strength characteristics of the material change. The values of the isentropic elastic moduli of shock-compressed material are determined from the relationship between the values measured in the experiments:

$$C_B = \sqrt{\frac{K_S}{\rho}}, \quad (7)$$

$$C_L = \sqrt{\frac{K_S + 4/3G}{\rho}}, \quad (8)$$

where C_B is bulk sound speed and C_L is longitudinal sound speed, K_S is isentropic bulk modulus, G is shear modulus.

To calculate the bulk sound speed, we use definition (2) in which the isentropic bulk modulus was calculated using few-parameter equation of state (EOS) from thermodynamic identity (9)

$$K_S = V \left[\frac{T}{c_v} \left(\frac{\partial P}{\partial T} \right)_V^2 - \left(\frac{\partial P}{\partial V} \right)_T \right]. \quad (9)$$

The results of the calculation of the bulk sound speed for different quantum mechanical theories [3–6] describing Grüneisen parameter and the experimental data are presented in figure 1 for copper and aluminum.

To calculate the longitudinal sound speed, we use preconditions of quantum-mechanical theory of Landau–Slater [3, 4], according to which the Poisson’s ratio remains constant when the pressure changes. Then, according to [10, 11], the sound longitudinal velocity can be calculated as

$$\frac{C_B}{C_L} = \sqrt{\frac{1 + \mu}{3(1 - \mu)}} \quad (10)$$

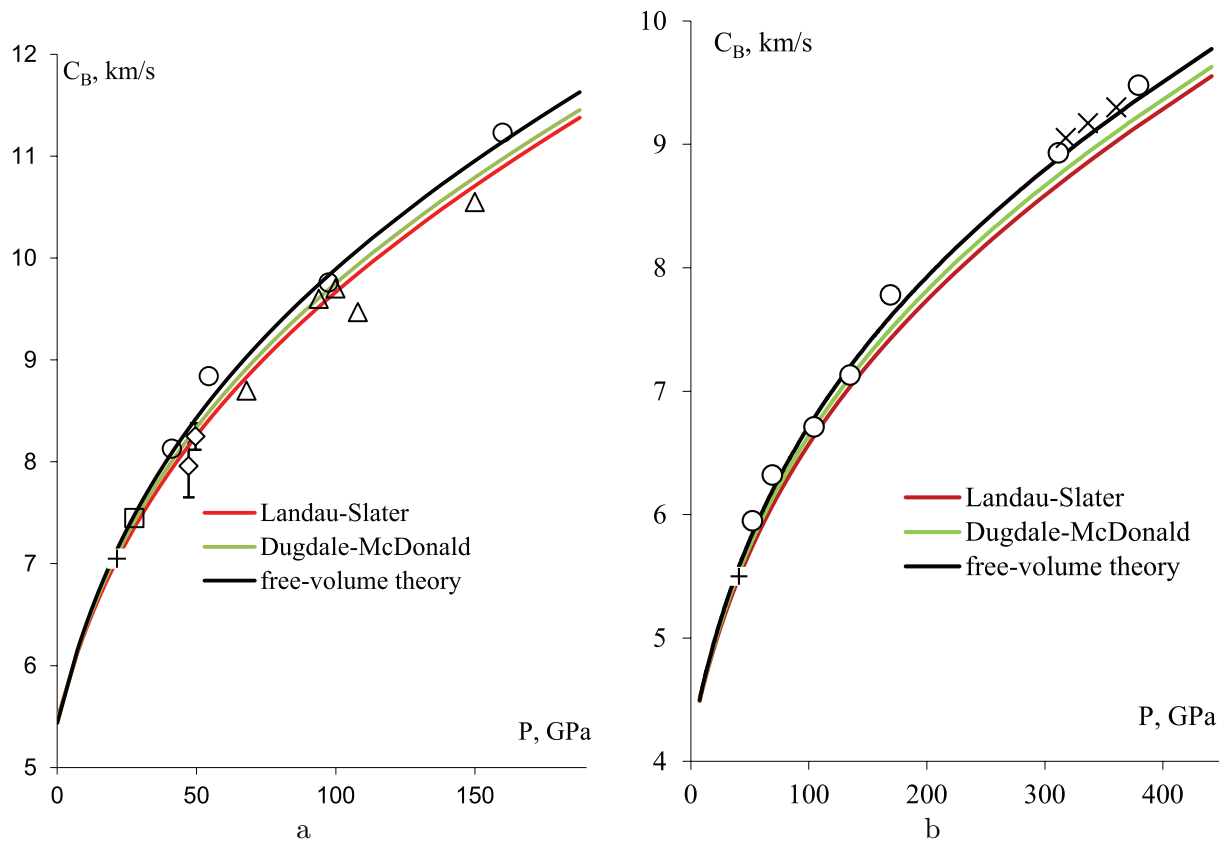


Figure 1. Dependence of the bulk sound speed on the pressure along the principal Hugoniot of (a) aluminum; (b) copper; experimental data: \circ —[10], $+$ —[12], \diamond —[13], \square —[14], \triangle —[15] \times —[16].

at that, Poisson's ratio is considered constant over the entire range of pressure variation and is equal to its initial value $\mu = \mu_0$.

Assuming the constancy of Poisson's ratio at the pressure variation, we limited ourselves to a single quantum-mechanical model, i.e., all the further calculations were performed only by the Landau-Slater model [3, 4]. The calculated longitudinal sound speed for aluminum and experimental data: aluminum [10, 13, 14], aluminum alloy Al-2024 [15, 17–20] and aluminum alloy LY12 [21, 22] are shown in figure 2. It can be seen from the figure that the simulation shows high accuracy in calculation of the values of the longitudinal sound speed with calculation error not exceeding 5% at pressures under 120 GPa. The pressure area over 120 GPa, which, according to numerous indirect evidences, corresponds to the molten aluminum, remains problematic. The fluid has no resistance to shear; therefore, the velocity of propagation of disturbances becomes equal to the bulk sound speed rather than the longitudinal one, as is observed in the experiments [15, 21].

Figure 3 shows the results of calculation and experimental data of the longitudinal sound speed for copper. A high precision of the speed of sound calculation by the few-parameter EOS is observed [25, 26]. The resulting accuracy of the calculation of the longitudinal and bulk sound speeds gives grounds to assert that the shear modulus calculated through the speed of sound by equation (3) and isentropic bulk modulus by (2) will have an error not exceeding 10%. As a confirmation of these words, figure 4 shows the calculated isentropic bulk modulus by the author's method for aluminum and copper, as well as the experimental data [10–16]. The error

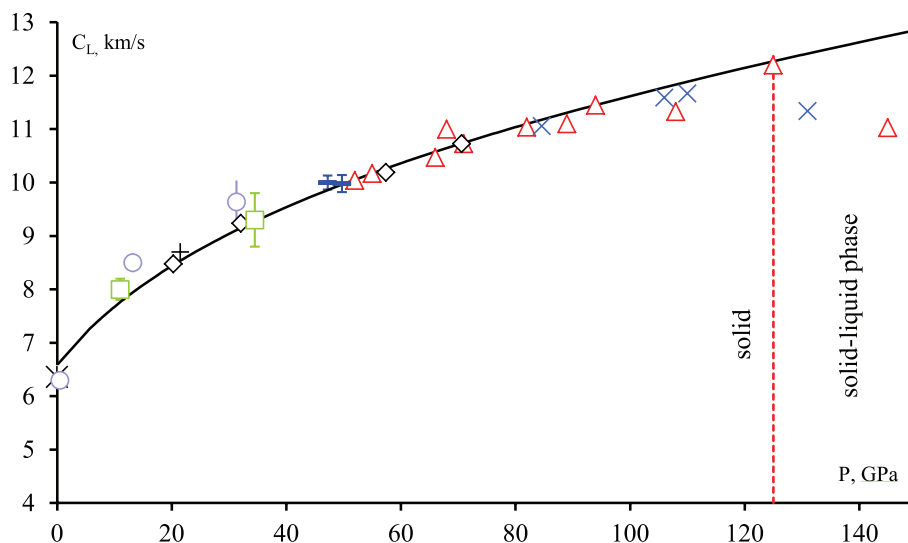


Figure 2. Longitudinal sound speed along the principal Hugoniot of aluminum; experimental data: *—[17], +—[12], —[13], Δ —[15], \bigcirc —[18,19], \square —[20], \times —[21], \diamond —[22].

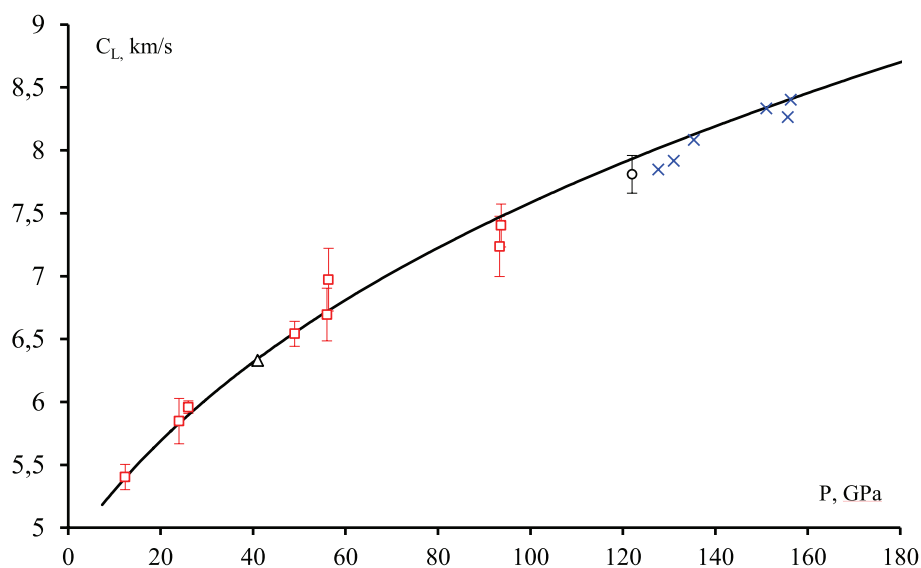


Figure 3. The longitudinal sound speed along the principal Hugoniot of copper; experimental data: \bigcirc —[11], Δ —[13], \square —[23], \times —[24].

of K_S calculation does not go beyond the stated error.

3. Dependence of the metal mechanical characteristics on variation of the temperature and pressure

Elasticity theory argues that in the case of homogeneous isotropic body, the elastic moduli are equal for all directions. Four elastic properties: Young's modulus, E , shear modulus, G , bulk modulus, K_S , and Poisson's ratio μ are interconnected. None of them can be measured directly in the shock-wave experiments. Each of these characteristics is expressed through elastic

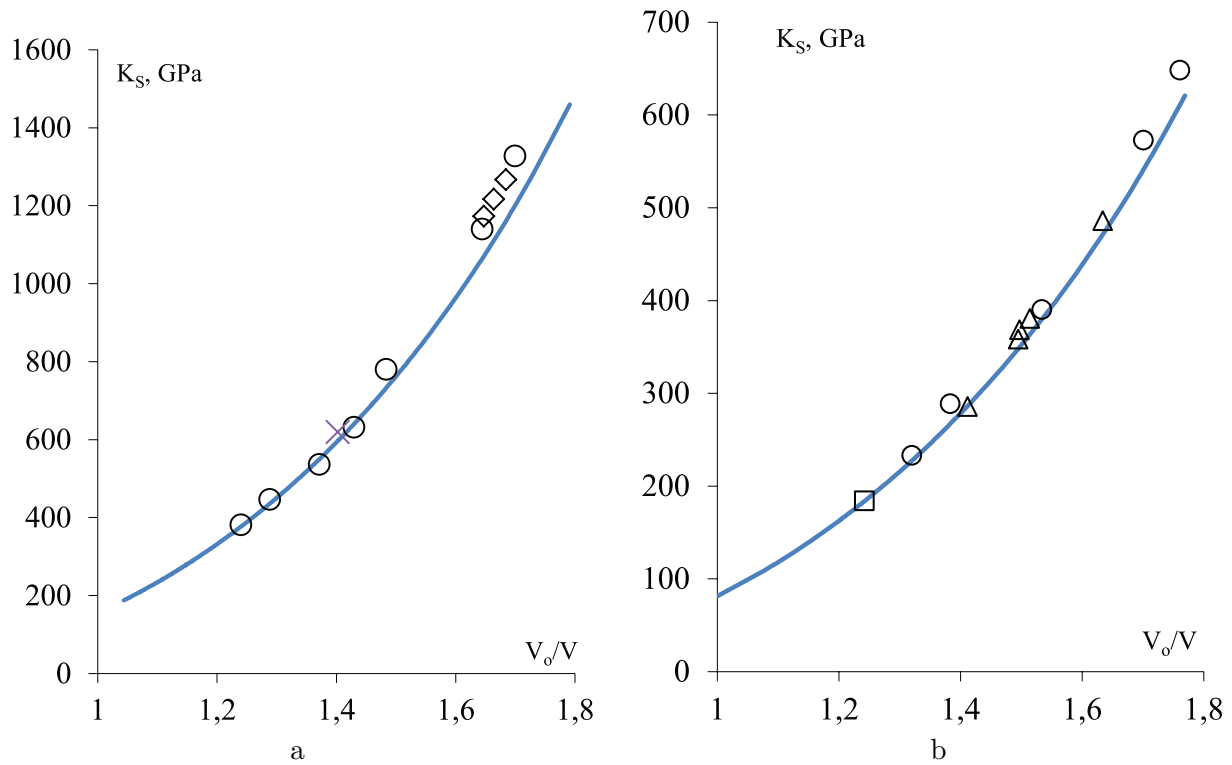


Figure 4. Bulk modulus on the principal Hugoniot of (a) aluminum and (b) copper; experimental data: \circ —[10], \times —[12], \square —[14], \triangle —[15], \diamond —[16].

longitudinal and bulk sound speeds

$$K_S = \rho C_B^2; \mu = \frac{3 - \left(\frac{C_L}{C_B}\right)^2}{3 + \left(\frac{C_L}{C_B}\right)^2};$$

$$E = \rho C_L^2 \frac{(1 - 2\mu)(1 + \mu)}{(1 - \mu)}; G = \frac{E}{2(1 + \mu)}. \quad (11)$$

All the elastic properties of homogeneous isotropic linear elastic materials are uniquely determined by any two moduli of elasticity. The others can be calculated by formulas of the theory of elasticity.

As indicated above, one of the modules of elasticity (isentropic bulk modulus) is determined with a high degree of accuracy. We consider the shear modulus as the second elastic characteristic. To date, there are numerous models for description of the shear modulus depending on the pressure and temperature. We will look at some of them.

3.1. MTS model of shear modulus

Chen-Gray model was created within MTS (mechanical threshold stress) plasticity model [27, 28], according to which the shear modulus is determined as

$$G(T) = G_0 - \frac{D}{e^{T_0/T} - 1}, \quad (12)$$

where G_0 and T_0 are initial values of the shear modulus and temperature, D is constant of the material.

This model is not used widely due to the absence of connection between the shear modulus and pressure. At that, it was shown experimentally [10, 29] that the shear modulus increases with increasing pressure and decreases with increasing temperature. Both pressure and temperature increase in the shock wave, and it is not clear from the model how these competing processes affect the shear modulus. Therefore, the only advantage of this model is simplicity of its implementation.

3.2. SCG model of shear modulus

The most famous model for description of the shear modulus is the model of Steinberg [30, 31]. This model is used by many researchers to simulate elastic-plastic flows in the solids. The shear modulus is a function of pressure and temperature

$$G(P, T) = G_0 \left(1 + A \frac{P}{\delta^{1/3}} - B (T - T_0) \right), \quad (13)$$

where G_0 is shear modulus under normal conditions $P = 0$, $T = T_0 = 300$ K, $\delta = \frac{V_0}{V}$ is compression, $A = \frac{1}{G_0} \frac{\partial G}{\partial P}$ and $B = \frac{1}{G_0} \frac{\partial G}{\partial T}$ are the constants of substance, which were selected by the authors for a large number of materials in [31, 32]. The basis for this was the results of the analysis of experimental data [33].

Unfortunately, this model has one significant drawback: it is assumed that when the temperature rises above the melting temperature, shear modulus turns instantaneously to zero, i.e., the shear modulus is presented by discontinuous function near the phase boundary.

3.3. NP model of shear modulus

Nadal-LePoac model [34] is an upgrade of the Steinberg model described above. In this model, the authors tried to eliminate one of the major drawbacks of the SCG model: the instantaneous change in the shear modulus at the melting point. Based on the Debye theory of solids and Linderman melting criterion, NP model helps to smooth the behavior of the shear modulus near the melting point:

$$G(P, T) = \frac{1}{\mathfrak{S}(\widehat{T})} \left[\left(G_0 + \frac{\partial G}{\partial P} \frac{P}{\delta^{1/3}} \right) (1 - \widehat{T}) + \frac{kT}{mCV} \right]; C = \frac{(6\pi^2)^{2/3}}{3} f^2, \quad (14)$$

$$\mathfrak{S}(\widehat{T}) = 1 + \exp \left(- \frac{1 + 1/\xi}{1 + \xi / (1 - \widehat{T})} \right), \text{ for } \widehat{T} = \frac{T}{T_m} \in [0, 1 + \xi],$$

where k is the Boltzmann constant, m is atomic weight, f is Linderman constant.

Despite the physically based approach, the model was not used widely in practice due to the complexity of its implementation.

3.4. BGP model of shear modulus

In [35, 36], Burakovsky proposed a new model of shear modulus depending on the volume and temperature. The model is based on the dislocation theory of phase transitions [37, 38] and the Debye theory of solids (in which the shear modulus is proportional to the square of the Debye temperature), using the Linderman criterion to determine the onset of melting:

$$G(\rho, T) = G(\rho, 0) \left(1 - \beta_b \frac{T}{T_m} \right), \quad (15)$$

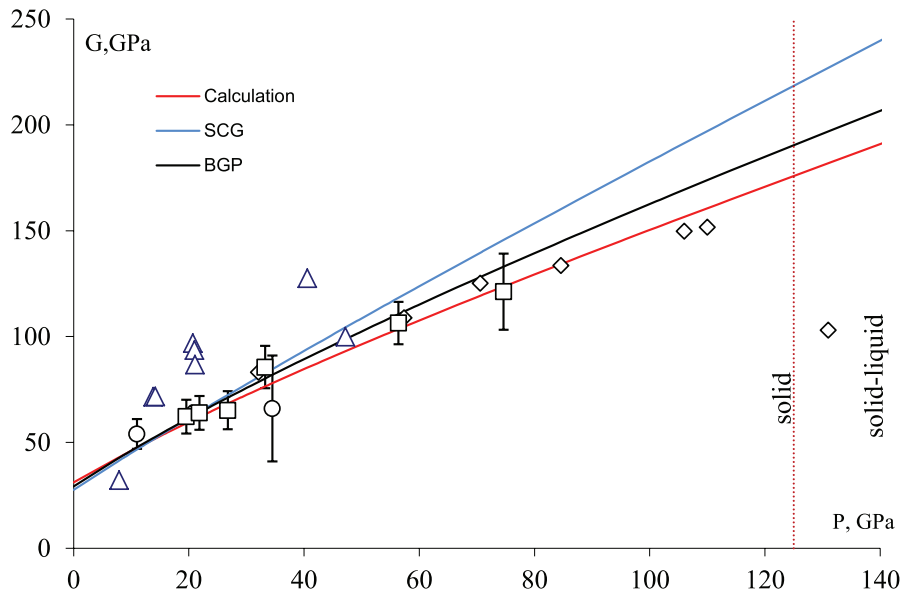


Figure 5. The shear modulus on the principal Hugoniot of aluminum; experimental data: \times —[15], \circ —[20], \diamond —[21, 22], \square —[40], \triangle —[41].

$$G(\rho, 0) = G(\rho_0, 0) \left(\frac{\rho}{\rho_0} \right)^{\frac{4}{3}} \exp \left\{ 6\gamma_1 \left(\frac{1}{\rho_0^{1/3}} - \frac{1}{\rho^{1/3}} \right) + \frac{2\gamma_2}{q} \left(\frac{1}{\rho_0^q} - \frac{1}{\rho^q} \right) \right\},$$

where β_b is constant of the material, γ_1, γ_2, q are constants for the Grüneisen equation in the form $\gamma = \frac{1}{2} + \frac{\gamma_1}{\rho^{1/3}} + \frac{\gamma_2}{\rho^q}$.

All the above models were successfully tested in practice, demonstrating an acceptable accuracy in the calculation of the shear modulus. However, these models have one major drawback: they require knowledge of additional specific constants, most of which are determined empirically. No above models are suitable for practical use in calculations, if the values of these specific constants (depending on the model) are not previously identified.

Such an approach is completely contrary to the philosophy of the few-parameter equation of state. Therefore, we formulate the problem: to determine the shear modulus of the material using the existing six constants of few-parameter EOS [1] and thermodynamic identities. Relying on the fact that the accuracy of calculation of the sound volume and longitudinal velocities is high enough, we calculate the shear modulus from ratio

$$G = \frac{3}{4} \frac{(C_L^2 - C_B^2)}{V}. \quad (16)$$

Figure 5 shows the calculation results of the shear modulus of aluminum depending on the pressure on the principal Hugoniot as described in (16) and by SCG (13), BSP (15) models. The constants for the Steinberg model ($G_0 = 27.6$ GPa, $A = 65$ TPa $^{-1}$; $B = -0.62$ kK $^{-1}$) were taken from [30], and for the Burakovsky model, we used dependence of the shear modulus of aluminum on the pressure $G(P, T = 0) = 29.3 \left(1 + \frac{P}{12.9} \right)^{0.79}$ [39]. For comparison, the experimental data and the results from paper [41] dedicated to processing of various experimental data on the speed of sound are also shown in figure 5. The author's solution is a bit different from the BSP (15) and SCG (13) models. Due to the significant scatter of the experimental data, one cannot

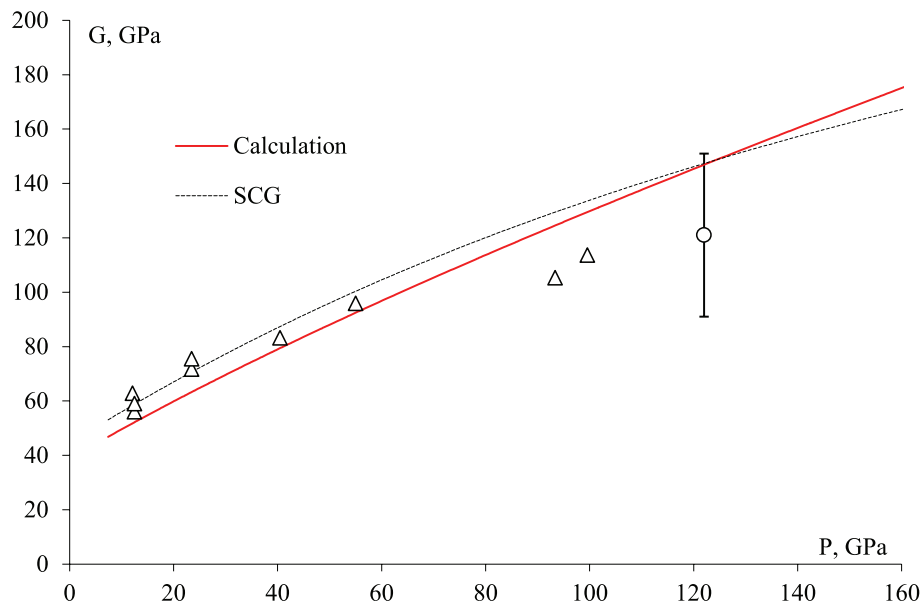


Figure 6. The shear modulus along the principal Hugoniot of copper; experimental data: \circ —[10], \triangle —[41].

identify which model is better. At that, it is necessary to take into account that the constants for SCG model (8) are chosen in [30] from the description of the experimental data in the low stress area, which gives only an approximate estimate of these values at the transition to high stresses (pressures).

The experimental data, due to their large scatter, cannot act as a criterion determining the correct calculation of the shear modulus by a particular model. Taking into account the fact that the shear modulus cannot be measured experimentally, one can argue that the crucial indicator of accuracy of the shear modulus calculation is the accuracy of measuring the both sound velocities at the same time. Meanwhile, it was shown above that the accuracy of calculation of the sound velocities by the few-parameter EOS is quite high.

Figure 6 shows the result of calculation of the shear modulus for copper along the principal Hugoniot. The result of calculation of the shear modulus by SCG model (13) is shown for comparison. Steinberg model constants are taken from [30] ($G_0 = 47.7$ GPa, $A = 28$ TPa $^{-1}$; $B = -0.38$ kK $^{-1}$). The author's calculation, though falls within the experimental interval under consideration, shows a tendency to overestimate the shear modulus at pressures more than 100 GPa. Apparently, this is due to the constancy of the Poisson's ratio assumed in the calculation. However, Poisson's ratio increases monotonically with increasing pressure from the initial value to the value of an incompressible fluid, $\mu = 0.5$, and that is not taken into account in our calculations.

4. Conclusions

In the paper, the existing models and methods for description of the temperature dependences of the elastic constants of materials are analyzed, and a relatively simple method for calculating the mechanical properties within the unified approach of the few-parameter equation of state is proposed. The error in calculation of the bulk modulus is less than 5%, the error in calculation of the mechanical values does not exceed 10–15% of the experimental data.

References

- [1] Fomin V M, Kraus E I and Shabalin I I 2004 *Mater. Phys. Mech.* **7** 23
- [2] Molodets A M, Shakhray D V, Golyshev A A, Babare L V and Avdonin V V 2006 *High Pressure Res.* **26** 223
- [3] Landau L D, Stanyukovich K P 1945 *Dokl. Phys.* **46** 399 (in Russian)
- [4] Slater I C 1939 *Introduction in the Chemical Physics* (New York: McGraw Hill Book Company)
- [5] Dugdale J S and McDonald D 1953 *Phys. Rev.* **89** 832
- [6] Vaschenko V Ya and Zubarev V N 1963 *Sov. Phys. Solid State*, **5** 653
- [7] Kraus E I, Fomin V M and Shabalin I I 2010 Few-parameter equation of state of the condensed matter and its application to the impact problems *EPJ Web of Conferences* **10** 00027
- [8] Kraus E I and Shabalin I I 2013 *Frattura ed Integrita Strutturale* **24** 138
- [9] Kraus E I, Lavrikov S V, Medvedev A E, Revuzhenko A F and Shabalin I I 2009 *J. Appl. Mech. Tech. Phys.* **50** 661
- [10] Altshuler L V, Kormer S B, Brazhnik M I, Vladimirov L A, Speranskaya M P and Funtikov A I 1960 *Sov. Phys. JETP* **11** 766
- [11] Vorob'ev A A, Dremine A N and Kanel' G I 1974 *J. Appl. Mech. Tech. Phys.* **5** 94
- [12] Altshuler L V 1965 *Usp. Fiz. Nauk* **85** 197
- [13] Asay J R, Chhabildas L C, Kerley G I and Trucano T G 1986 High pressure strength of shocked aluminum *Shock Waves in Condensed Matter* ed Y M Gupta (New York: American Institute of Physics) pp 145–149
- [14] Neal T 1976 *J. Appl. Phys.* **46** 2521
- [15] McQueen R G, Fritz J N and Morris C E 1984 The velocity of sound behind strong shock waves in 2024 Al *Shock Waves in Condensed Matter* ed J R Asay, R A Graham and G K Straub (Amsterdam: North Holland) pp 95–98
- [16] Hayes D, Hixson R S and McQueen R G 2000 High pressure elastic properties, solid-liquid phase boundary and liquid equation of state from release wave measurements in shock-loaded copper *Shock Compression of Condensed Matter* ed M D Furnish, L C Chhabildas and R S Hixson (New York: American Institute of Physics) pp 483–488
- [17] Marsh S P 1980 *LASL Shock Hugoniot Data* (University of California Press)
- [18] Kusubov A S and van Thiel M 1969 *J. Appl. Phys.* **40** 3776
- [19] Kusubov A S and van Thiel M 1969 *J. Appl. Phys.* **40** 893
- [20] Erkman J O and Christensen A B 1967 *J. Appl. Phys.* **38** 5395
- [21] Yu Y Y, Tan H, Hu J B and Dai C D 2008 *Chinese Phys. B* **17** 264
- [22] Yu Y Y, Tan H, Dai C D, Hu J B and Chen D N 2005 *Chinese Phys. Lett.* **22** 1742
- [23] Chhabildas L C and Asay J R 1981 *Proc. 8th AIRAPT Conf. (Uppsala)* (Sweden: Uppsala University) p 183
- [24] Hu J B, Jing F Q, Cheng J X 1989 *Chinese Journal of High Pressure Physics* **3** 187
- [25] Buzyurkin A E, Kraus E I and Lukyanov Ya L 2013 *Frattura ed Integrita Strutturale* **24** 102
- [26] Kraus E I, Fomin V M and Shabalin I I 2011 *Proc. 11th Int. Conf. on Computational Science and Its Applications (Santander)* (IEEE Computer Society) p 239
- [27] Chen S R and Gray G T 1996 *Metall. Mater. Trans.* **27** 2994
- [28] Goto D M, Bingert J F, Reed W R and Garrett R K 2000 *Scripta Mater.* **42** 1125
- [29] Abey A E 1971 *J. Appl. Phys.* **42** 4085
- [30] Steinberg D J, Cochran S G and Guinan M W 1980 *J. Appl. Phys.* **51** 1498
- [31] Steinberg D J and Lund C M 1989 *J. Appl. Phys.* **65** 1528
- [32] Steinberg D J 1996 *LLNL Report No. UCRL-MA-106439*
- [33] Guinan M W and Steinberg D J 1974 *J. Phys. Chem. Solids* **35** 1501
- [34] Nadal M H and Le Poac P 2003 *J. Appl. Phys.* **93** 2472
- [35] Burakovsky L, Greeff C W and Preston D L 2003 *Phys. Rev. B* **67** 094107
- [36] Burakovsky L and Preston D L 2006 *J. Phys. Chem. Solids* **67** 1930
- [37] Burakovsky L and Preston D L 2000 *Solid State Commun.* **115** 341
- [38] Burakovsky L, Preston D L and Silbar R R 2000 *Phys. Rev. B* **61** 15011
- [39] Burakovsky L and Preston D L 2005 *Phys. Rev. B* **71** 184118
- [40] Hu J B, Yu Y Y, Tan H and Dai C D 2006 *Chinese Phys. Lett.* **23** 1265
- [41] Peng J, Jing F, Li D and Wang L 2005 *J. Appl. Phys.* **98** 013508